

Generalized fractal dimensions of laser Doppler flowmetry signals recorded from glabrous and nonglabrous skin

Benjamin Buard^{a)}

*Groupe ESAIP, 18 rue du 8 mai 1945, BP 80022, 49180 Saint Barthélemy d'Anjou Cedex, France
and Laboratoire d'Ingénierie des Systèmes Automatisés (LISA), Université d'Angers, 62 Avenue Notre Dame du Lac, 49000 Angers, France*

Guillaume Mahé

*Laboratoire de Physiologie et d'Explorations Vasculaires, UMR CNRS 6214-INSERM 771,
Centre Hospitalier Universitaire d'Angers, 49033 Angers Cedex 01, France*

François Chapeau-Blondeau and David Rousseau

Laboratoire d'Ingénierie des Systèmes Automatisés (LISA), Université d'Angers, 62 Avenue Notre Dame du Lac, 49000 Angers, France

Pierre Abraham

*Laboratoire de Physiologie et d'Explorations Vasculaires, UMR CNRS 6214-INSERM 771,
Centre Hospitalier Universitaire d'Angers, 49033 Angers Cedex 01, France*

Anne Humeau

Laboratoire d'Ingénierie des Systèmes Automatisés (LISA), Université d'Angers, 62 Avenue Notre Dame du Lac, 49000 Angers, France

(Received 13 November 2009; revised 26 February 2010; accepted for publication 22 March 2010; published 21 May 2010)

Purpose: The technique of laser Doppler flowmetry (LDF) is commonly used to have a peripheral view of the cardiovascular system. To better understand the microvascular perfusion signals, the authors herein propose to analyze and compare the complexity of LDF data recorded simultaneously in glabrous and nonglabrous skin. Glabrous zones are physiologically different from the others partly due to the presence of a high density of arteriovenous anastomoses.

Methods: For this purpose, a multifractal analysis based on the partition function and generalized fractal dimensions computation is proposed. The LDF data processed are recorded simultaneously on the right and left forearms and on the right and left hand palms of healthy subjects. The signal processing method is first tested on a multifractal binomial measure. The generalized fractal dimensions of the normalized LDF signals are then estimated. Furthermore, for the first time, the authors estimate the generalized fractal dimensions from a range of scales corresponding to factors influencing the microcirculation flow (cardiac, respiratory, myogenic, neurogenic, and endothelial).

Results: Different multifractal behaviors are found between normalized LDF signals recorded in the forearms and in the hand palms of healthy subjects. Thus, the variations in the estimated generalized fractal dimensions of LDF signals recorded in the hand palms are higher than those of LDF signals recorded in the forearms. This shows that LDF signals recorded in glabrous zones may be more complex than those recorded in nonglabrous zones. Furthermore, the results show that the complexity in the hand palms could be more important at scales corresponding to the myogenic control mechanism than at the other studied scales.

Conclusions: These findings suggest that the multifractality of the normalized LDF signals is different on glabrous and nonglabrous skin. This difference may rely on the density of arteriovenous anastomoses and differences in nerve supply or biochemical properties. This study provides useful information for an in-depth understanding of LDF data and a more detailed knowledge of the peripheral cardiovascular system. © 2010 American Association of Physicists in Medicine.

[DOI: [10.1118/1.3395577](https://doi.org/10.1118/1.3395577)]

Key words: laser Doppler flowmetry, multifractal analysis, partition function, generalized dimension, glabrous skin, microcirculation, spatial variation, biomedical engineering

I. INTRODUCTION

The peripheral cardiovascular system can be studied with the laser Doppler flowmetry (LDF) method. LDF is a well-known technique for assessing tissue microcirculation in a continuous and noninvasive way.¹ It is now established for the real-time monitoring of microvascular perfusion in tissue

and is commonly used in clinical research.^{2,3} This technique is based on the Doppler effect generated by the interactions between photons of a laser light and moving scatterers, mainly red blood cells of the microcirculation. Both concentration and velocity of the moving scatterers affect the LDF perfusion estimate.⁴

Hand palms and forearms do not possess the same physiological properties. Glabrous skin blood flow is controlled solely by a tonic vasoconstrictor system. In contrast, nonglabrous skin blood flow is governed by both a sympathetic vasoconstrictor system and a separate sympathetic active vasodilator system.⁵ In addition to neural controls, a number of other local factors are also capable of modulating skin blood flow. Moreover, one of the important differences in microcirculatory system of glabrous and nonglabrous skin is the presence of arteriovenous anastomoses (AVAs). An AVA is a blood vessel that connects an arteriole directly to a venule without capillary intervention. Glabrous skin contains both surface capillary loops and deeper AVAs, while nonglabrous skin contains capillary loops but lacks AVAs.⁶ AVAs provide an efficient thermal regulation⁷ and cause large fluctuations in skin blood flow.⁸ Neither these fluctuations in blood flow through the AVAs nor the AVA architecture is present to any significant degree in nonglabrous skin.⁹

Some studies using LDF monitors have already underlined differences between glabrous and nonglabrous zones.^{10–12} For example, it has been shown that a dynamic exercise decreases in an intensity-dependent manner, via an adrenergic vasoconstrictor pathway, the sensitivity for thermal vasodilatation in glabrous skin but not in nonglabrous skin.¹² Furthermore, the sweating response from nonglabrous skin (chest, forearm, and thigh) increases linearly with increasing exercise intensity, whereas glabrous skin (palm) does not show a clearly graded response.¹⁰ Last, another study has shown that glabrous skin of the palm buffers blood flow oscillations induced by changes in arterial blood pressure, thereby demonstrating dynamic autoregulatory capabilities that appear to be absent or attenuated in nonglabrous skin of the forearm.¹¹ However, none of these studies have analyzed glabrous and nonglabrous zones, observing LDF signals complexity.

The goal of our paper is to compare the complexity of the LDF data in glabrous and nonglabrous zones. For this purpose, a multifractal analysis of LDF signals recorded simultaneously in forearms and hand palms is performed. Recent works have shown that LDF recordings from the forearm of young healthy subjects are weakly multifractal,¹³ but that aging can lead to a reduced multifractality.¹⁴ We herein propose a multifractal analysis through the computation of the signal partition functions and the estimation of their generalized fractal dimensions.

II. LDF TECHNIQUE

LDF allows a continuous monitoring of microcirculatory blood flow. The technique relies on the Doppler shift. A coherent light is steered toward a tissue, through a fiber optics. Photons sent in this way are backscattered by static or in-movement structures. When they meet moving particles, mainly red blood cells, light undergoes changes in wavelength due to the Doppler shift. The magnitude and frequency distribution of these changes in wavelength are re-

lated to the number and velocity of the blood cells. The backscattered light is brought toward an optical fiber to a photoreceptor.

LDF enables the evaluation of cutaneous microvascular blood flow over time and its alterations with little or no influence on physiologic blood flow. The major advantage of this noninvasive technique is its sensitivity at detecting and quantifying relative changes in the skin blood flow in response to a given stimulus. The output value constitutes the flux of red cells, defined as the number of red blood cells in the floodlighted volume times their velocity, and is reported as microcirculatory perfusion units (with arbitrary units, a.u.). The relationship between the flowmeter output signal and the flux of red blood cells is linear. The beam can penetrate, tissue to a depth of 1–2 mm (depending among others on the wavelength of the laser and the place of the probe). LDF is presently a very common technique in clinical research and has a lot of clinical applications.^{2,15}

On the time scale of minutes, different subsystems can be considered to contribute to the regulation of the blood flow.¹⁶ Under stationary conditions, when a healthy subject is at physical and mental pause, some authors found six characteristic frequencies in LDF signals, linked to different “factors influencing the microcirculation flow (FIMF):”^{17,18} Around 1.1 Hz for the heart beats, 0.36 Hz for the respiration, 0.1 Hz for the myogenic mechanisms, 0.04 Hz for the neurogenic mechanisms, and 0.01 Hz for the nitric oxide (NO) endothelial-related metabolic mechanisms. The sixth characteristic frequency as recently been found at 0.007 Hz and is supposed to be related to non-NO-dependent endothelium mechanisms, such as endothelium-derived hyperpolarizing factor (EDHF).¹⁷ The characteristic frequency values are different from subject to subject, but are found in the same frequency intervals for all subjects.¹⁸

The heartbeat (around 1.1 Hz) and respiration oscillations can be selectively observed and are relatively well understood. The heart’s pumping activity is manifested in every single vessel and is also present in the microcirculation through the capillary bed.¹⁹ The characteristic frequency around 0.36 Hz has been observed on respiratory signals and is known to be the breathing frequency.¹⁹ For the other characteristic frequencies, only indirect evidence is available. The characteristic frequency observed at around 0.1 Hz is thought to represent the intrinsic myogenic activity of the vascular smooth muscles, caused by the pacemaker cells found within the vessel walls.²⁰ On isolated vessels, myogenic origin of this oscillation has been demonstrated both by measuring dynamic vessels diameter changes²¹ and ion concentration.²² The activity of the nervous system serves to maintain a basal level of contraction of the vessels. Without additional influences, this function is oscillatory.¹⁹ The characteristic frequency at around 0.04 Hz is hypothesized, due to indirect evidence, to originate from neurogenic control mechanism.²³ This oscillation disappears after denervation. Moreover, significantly lower oscillations have been observed on flaps of transplanted skin compared to intact skin.²⁴ Using acetylcholine and sodium nitroprusside, indirect evidence has shown the endothelial origin of the char-

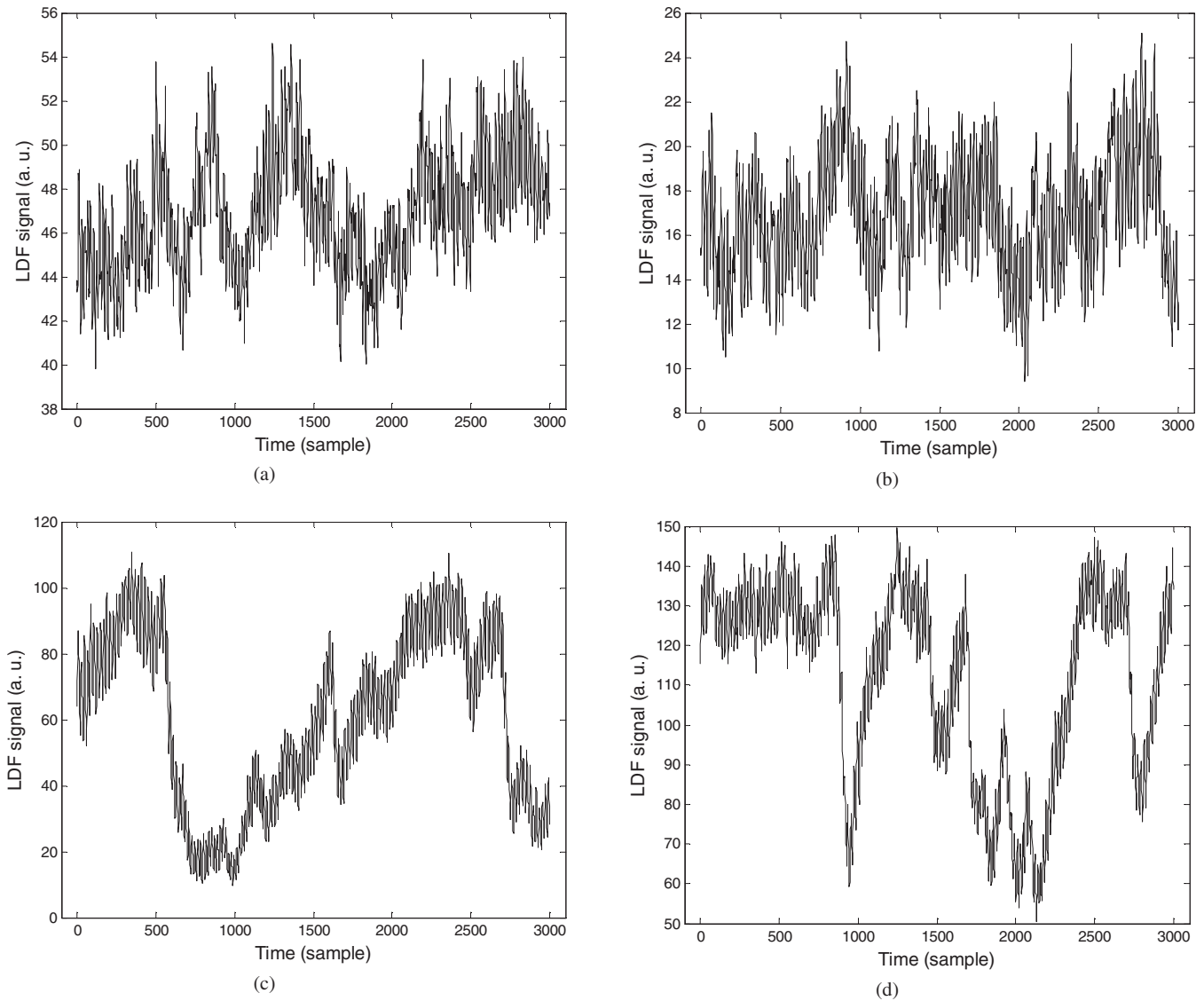


FIG. 1. LDF signals recorded (a) in the right forearm, (b) in the left forearm, (c) in the right hand palm, and (d) in the left hand palm of a young healthy subject (29 yr old) in a supine position.

acteristic frequency at around 0.01 Hz.²⁵ Moreover, it has been shown that the endothelial dependency of this oscillation is, at least partly mediated, by NO.²⁶ However, inhibition of NO or prostaglandin synthesis does not affect the endothelial dependency of the last characteristic frequency found at around 0.007 Hz.¹⁷ Thus, other endothelial mechanisms, such as EDHF, might be involved and attributed to this latter low frequency.

III. MEASUREMENT PROCEDURE

For our signal processing analysis, the measurement procedure for the LDF signals was conducted in accordance with the Declaration of Helsinki and is as follows: Eight healthy subjects were studied in the supine position. Their mean age was 30.8 ± 12.2 yr. All subjects gave their written informed consent to participate. None of them had a history of hypertension, hypotension, diabetes mellitus, vascular disease, or showed any evidence of disease at the time of the

study. The measurements were performed in a quiet room with an ambient temperature set at 24 ± 1 °C. The subjects were asked not to talk or to move during the experiments in order to avoid any signal disturbances. After at least 10 min of acclimatization, skin blood flow measurement started. For this purpose, four LDF probes (PF408, Perimed, Stockholm, Sweden), connected to two laser Doppler flowmeters (Perimed, Stockholm, Sweden), were used. One LDF probe was positioned on each forearm (ventral face) of the subjects. Two other probes were positioned, one on each hand palm. As suggested by the manufacturer, the time constants of the laser Doppler flowmeters were set to 0.2 s. Skin blood flow was assessed in a.u. and recorded on a computer via an analog-to-digital converter (Biopac System, Goleta, CA) with a sample frequency of 20 Hz. Four LDF signals were thus recorded simultaneously for each subject. LDF signals recorded from one subject are shown in Fig. 1. In what follows, we analyze 3000 samples from each LDF signal.

IV. MULTIFRACTAL ANALYSIS

The concept of multifractality and its formalism have been developed by many²⁷⁻²⁹ authors and applied to several fields of the scientific research. Recently, multifractal analysis has been used for the study of physiological signals.^{30,31} The multifractal formalism is based on the partition function, which is defined as (details can be found in Ref. 32)

$$Z(q, \varepsilon) = \sum_{i=1}^{N_{\text{boxes}}(\varepsilon)} \mu_i(\varepsilon)^q, \tag{1}$$

where ε is the size or scale of the boxes used to cover the sample. The exponent q is a continuous real parameter, playing the role of the moment order of the measure $\mu_i(\varepsilon)$. $N_{\text{boxes}}(\varepsilon)$ indicates the number of boxes of size ε needed to cover the sample. The measure $\mu_i(\varepsilon)$ can be seen as a probability, so we have

$$\sum_i \mu_i(\varepsilon) = 1. \tag{2}$$

The parameter q can be considered as a powerful microscope and a selective parameter.³³ Choosing large value of q favors boxes with high values of $\mu_i(\varepsilon)$. Conversely, low values of q favor boxes with low values of the measure. That is why, when changing the value of q , different parts of the measure probability distribution are explored. In the same way, a change in the box size (ε) allows one to explore the signal at different scales. Therefore, the partition function supplies information at different scales.

The generalized fractal dimensions are defined by the asymptotic behavior of the ratio between $\ln(Z(q, \varepsilon))$ and $\ln(\varepsilon)$,²⁹

$$D(q) = \lim_{\varepsilon \rightarrow 0} \frac{1}{q-1} \frac{\ln(Z(q, \varepsilon))}{\ln(\varepsilon)}, \tag{3}$$

where D_0 is the fractal dimension of the support of the measure and D_2 corresponds to the correlation dimension.²⁹ Applying l'Hôpital's rule in Eq. (3), we get³⁴

$$D_1 = \lim_{\varepsilon \rightarrow 0} \frac{\sum_i \mu_i \ln(\mu_i)}{\ln(\varepsilon)}, \tag{4}$$

where D_1 is called the information dimension. The higher $D(q)$ are related to higher correlations on the measure.²⁹

A signal with a constant $D(q)$ is a monofractal signal, i.e., it is homogeneous and has the same scaling properties throughout its length.³⁵ On the contrary, a multifractal signal is nonlinear and inhomogeneous with local properties changing with time. Such a signal requires many exponents to fully characterize its properties.³² Thus, when the value of D depends on q , the signal is considered as multifractal. In this case, $D(q)$ usually decreases with increasing q .

In most practical applications, the limit in Eq. (3) cannot be calculated either because no information is available at small scales or because no scaling can exist below a mini-

mum physical length.³³ This drawback can be overcome using a scaling region where a power law can be fitted to the partition function. We then obtained

$$Z(q, \varepsilon) \propto \varepsilon^{\tau(q)}, \tag{5}$$

where the slope $\tau(q)$ is related to the generalized fractal dimensions by

$$\tau(q) = (q - 1)D(q). \tag{6}$$

In what follows, we first check our multifractal analysis on a binomial measure, which is a multifractal signal with known properties. We then estimate the generalized fractal dimensions of our 32 LDF signals recorded in glabrous and nonglabrous zones of our eight healthy human subjects. To be as close as possible to the limit defined in Eq. (3), we first estimated the generalized fractal dimensions for small boxes size in the order of the sample duration. We then selected the box sizes in accordance with some FIMF (see below).

V. MULTIFRACTAL ANALYSIS OF A BINOMIAL MEASURE

We first propose to apply the abovementioned processing steps on a binomial measure. A binomial measure is generated recursively with a multiplicative cascade. This cascade starts ($k=0$) with a uniformly distributed unit of mass on the unit interval $I=I_0=[0, 1]$. At the next stage ($k=1$), this measure is divided into two equal parts with uniformly distributed mass on each part. We thus obtain fraction m_0 on the interval $I_0=[0, 1/2]$ and $m_1=1-m_0$ on the interval $I_1=[1/2, 1]$. This operation can then be iterated until the desired order. We obtain³⁶

$$\tau(q) = -\log_2(m_0^q + m_1^q). \tag{7}$$

The generalized fractal dimensions can then be obtained with Eq. (6).

We herein process a binomial measure with $m_0=0.650$, $m_1=0.350$, and $k=11$. The results are shown in Figs. 2 and 3. We can observe that the partition function has a power-law behavior for all scales (see Fig. 2) as awaited for such a signal.³¹ Moreover, $Z(1, \varepsilon)=1$ at each scale, which is in accordance with Eq. (2). We can also see that the numerically estimated generalized fractal dimensions are very similar to the theoretical one (see Fig. 3). These results validate our numerical evaluation process of the generalized fractal dimensions.

Furthermore, the role played by the signal's amplitude has been studied. Thus, the generalized fractal dimension of a binomial measure similar to the one described above (which has a mean value of around 0.0005), but having a mean value of 80, has been estimated (see Fig. 4). Comparing Figs. 3 and 4, we can observe that the generalized fractal dimension obtained for the latter is clearly flatter than the original one. This phenomenon can be explained due to the fact that an increase in the mean value of a signal decreases its local variations and therefore its complexity.

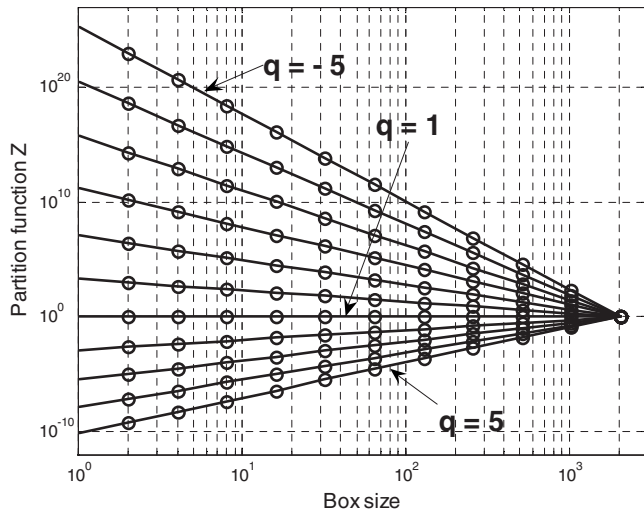


FIG. 2. Partition function of a binomial measure computed with $m_0=0.650$, $m_1=0.350$, and $k=11$.

VI. MULTIFRACTAL ANALYSIS OF LDF SIGNALS

Equation (2) implies to divide the processed signal by the sum of its samples' amplitude in order to obtain a measure. However, LDF signals are recorded in a.u. and their amplitudes are therefore intrinsically relative. As a consequence, in order to compare their complexity and to focus on their variations, we apply amplitude normalization on all our LDF signals before the multifractal analysis. We thus choose to normalize the analyzed signals to 80 a.u. (chosen arbitrarily).

The partition functions obtained in this way, with LDF signals recorded simultaneously in the forearms and the hand palms of a young healthy subject, are shown in Fig. 5. In this study, the q parameter varies between -5 and 5 and the size of the boxes are the divisors of 3000. We can observe that $Z(1, \varepsilon)=1$ at each scale. This is in accordance with Eq. (2). At first, to be closed to Eq. (3), we estimate the generalized

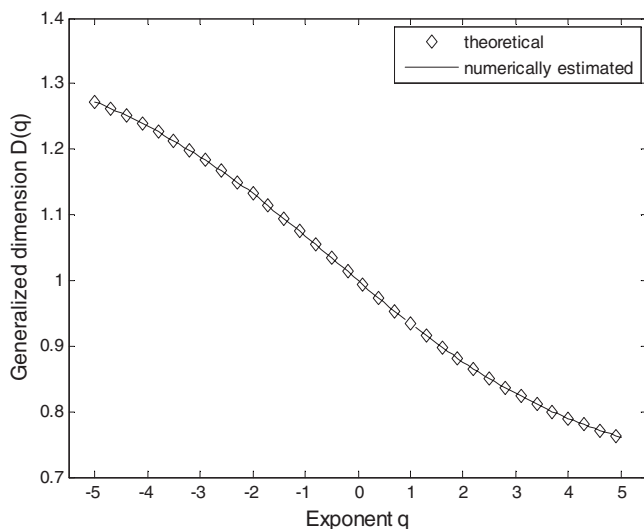


FIG. 3. Theoretical and numerically estimated generalized fractal dimensions of a binomial measure computed with $m_0=0.650$, $m_1=0.350$, and $k=11$.

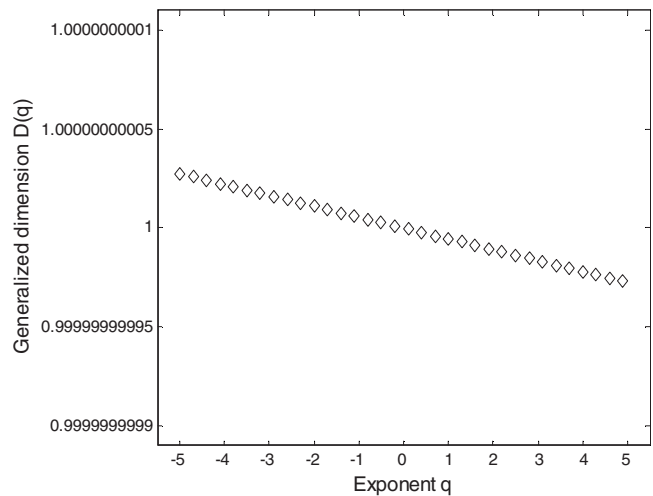


FIG. 4. Numerically estimated generalized fractal dimensions of a binomial measure computed with $m_0=0.650$, $m_1=0.350$, and $k=11$ and with a mean value of 80.

fractal dimensions with boxes of size between 1 and 3 samples. At these scales, a power law can be fitted to the partition function (see Fig. 5).

Figure 6 shows the average generalized fractal dimensions obtained from the normalized LDF signals recorded in the forearms and hand palms of the eight subjects with box sizes between 1 and 3 samples. We can observe that, in all cases, $D(0)=1$ as expected for a one dimension function. Furthermore, we can see that the generalized fractal dimensions obtained with the LDF signals recorded in the forearms are flatter than those obtained with the LDF signals recorded in the hand palms. This means that, at these scales, the normalized LDF signals recorded in the hand palms may be more complex than those recorded in the forearms. The latter signals, after amplitude normalization, exhibit properties almost similar to that of monofractal signals.

Observation of Eqs. (3) and (4) could lead to the conclusion that the generalized fractal dimension must be observed only on box sizes which would tend toward zero. However, the fractal dimension has already been generalized to be dependent on observation scales since its conception, with the use of the term "effective dimension."³² Its intuitive idea has been expressed to random walks³⁷ and the scale-dependent fractal dimension can already be useful to describe some chemical reaction rates.³⁸ That is why we now propose to estimate the generalized fractal dimensions of our LDF signals on different scales. For this purpose, we choose different boxes sizes in accordance with the six FIMF mentioned previously: The heart rhythm (between 0.6 and 2 Hz), the respiratory rhythm (0.145–0.6 Hz), the myogenic mechanisms (0.052–0.145 Hz), the neurogenic mechanisms (0.021–0.052 Hz), the NO endothelial-related metabolic mechanisms (0.0095–0.021 Hz), and the non-NO-dependent endothelium (0.005–0.0095 Hz) mechanisms. Due to our frequency sampling (20 Hz), we choose our box sizes as follows: Between 10 and 30 samples (0.6–2 Hz) to estimate the generalized fractal dimensions at the scales of the cardiac rhythm, be-

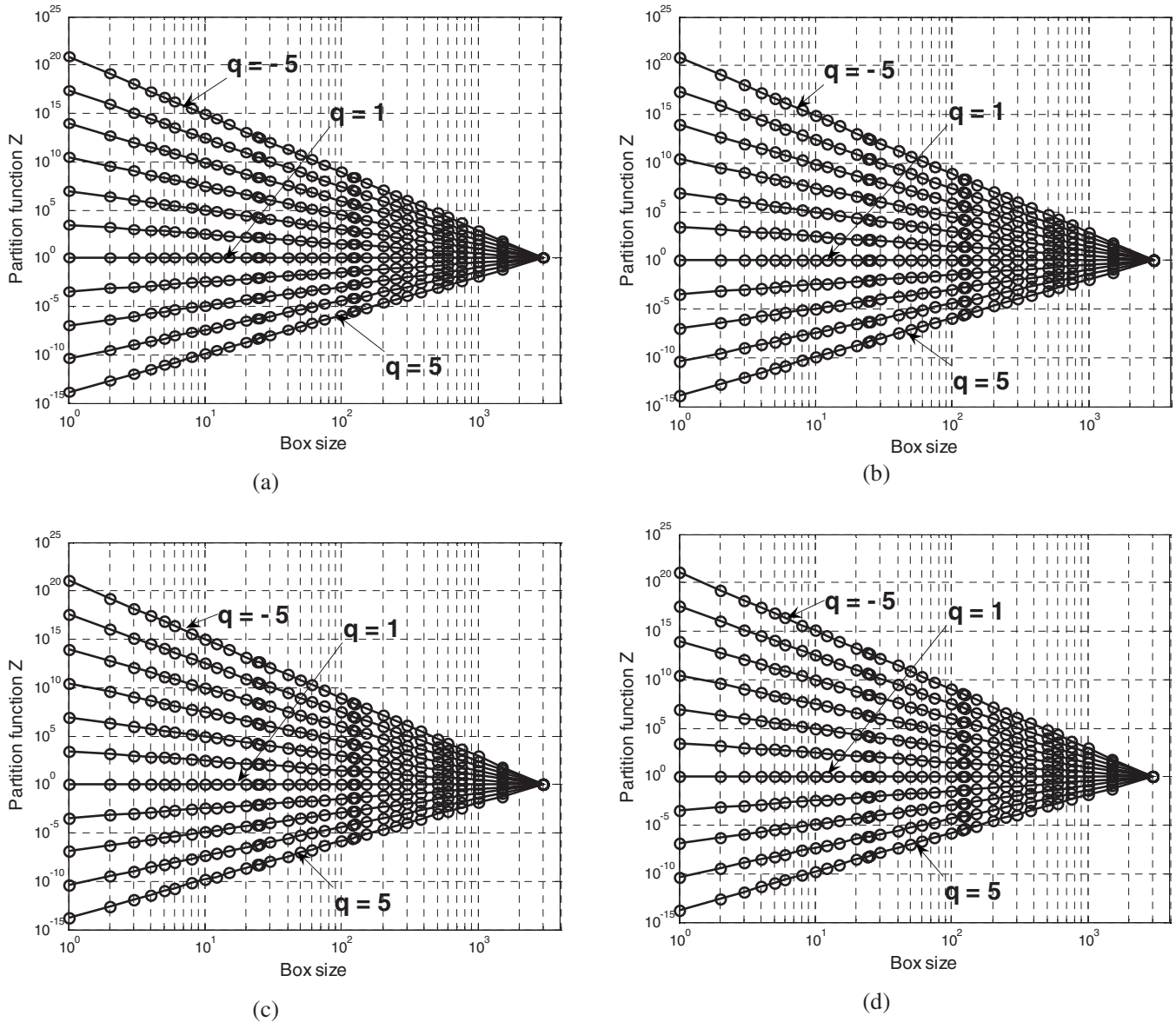


Fig. 5. Partition function of the normalized LDF signals recorded in (a) the right forearm, (b) the left forearm, (c) the right hand palm, and (d) the left hand palm of a young healthy subject (29 yr old) in a supine position. The q parameter varies between -5 and 5 . The size of the boxes varies between 1 and 3000 samples.

tween 30 and 125 samples (0.16 – 0.6 Hz) for the respiratory rhythm, between 125 and 375 samples (0.05 – 0.16 Hz) for the myogenic mechanisms, between 375 and 1000 samples (0.02 – 0.05 Hz) for the neurogenic mechanisms, and between 1000 and 3000 samples (0.006 – 0.02 Hz) for NO and EDHF related endothelial mechanisms.

A zoom of the partition function for a young healthy subject at each specific scale is shown in Fig. 7. We can see that for all scale regions, a power law can be fitted to the partition function.

The average generalized fractal dimensions, obtained on the normalized LDF signals recorded in the forearm (nonglabrous zone) and the hand palm (glabrous zone) for the eight healthy subjects at rest, are shown in Fig. 8. We can observe differences between the generalized fractal dimensions for each scale region. Furthermore, the relationship be-

tween the curvature of the generalized fractal dimensions and the scale region is not the same for the forearms [Figs. 8(a) and 8(b)] and the hand palms [Figs. 8(c) and 8(d)]. Thus, for the LDF signals recorded in the forearms (right and left), the generalized fractal dimensions which seem the most curved are, in decreasing order, related to the respiration and myogenic mechanisms (very close), the heart rhythm, the neurogenic mechanisms, and the endothelial mechanisms. For hand palm signals, the flattest generalized fractal dimensions are those related to the cardiac rhythm and the most curved are those related to the myogenic mechanisms. On both right and left hands [Figs. 8(c) and 8(d)], the estimated generalized fractal dimensions related to the neurogenic and to the endothelial mechanisms are very close.

Moreover, our results show that the estimated generalized fractal dimensions of normalized LDF signals recorded in

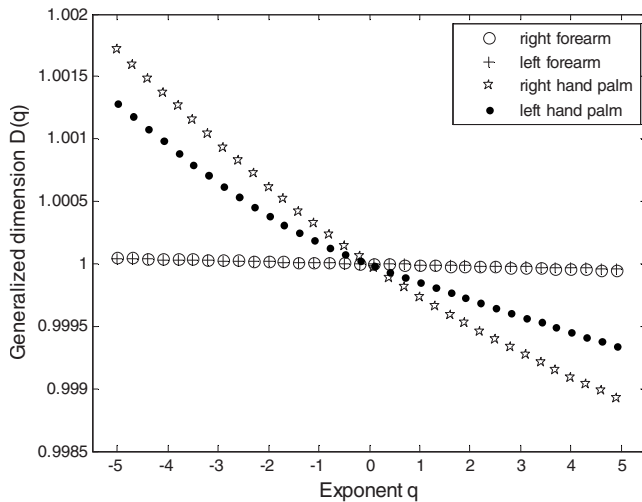


FIG. 6. Average generalized fractal dimensions obtained with the normalized LDF signals recorded in the right forearm, in the left forearm, in the right hand palm, and in the left hand palm of healthy subjects in a supine position. The signals have 3000 samples. The q parameter varies between -5 and 5 . The size of the boxes varies between 1 and 3 samples.

the right and left forearms are very similar, more than those obtained with the records in the left and right hand palms, whatever the scales. The spatial variations are thus more important on the hand palms than on the forearms.

From our results, we also show that the normalized LDF signals recorded in the hand palms of healthy subjects at rest may be more multifractal than those recorded in the forearms. This is in accordance with previous works using another method.^{31,39} Moreover, this study shows that, contrary to pure multifractal signals, like binomial measures, the scale chosen for the multifractal analysis of an experimental LDF signal has an impact on the estimated generalized fractal dimensions. In addition, the spatial variations and the low variations for the estimated generalized fractal dimensions at the scales corresponding to the cardiac regulating mechanisms in the hand palms tend to indicate that the possible multifractal properties of the LDF signals are not principally governed by a central command, predominant in these zones. Moreover, the estimated generalized fractal dimensions of LDF signals recorded in the hand palms (for both sides) are the most curved at the scales corresponding to the myogenic regulating mechanisms. This control mechanism is connected to the vessels, which contribute to control the flow of blood via the mechanism named myogenic autoregulation. We have previously seen that one of the main differences in the skin blood flow between hand palms and forearms is the presence of blood vessels that connect directly arterioles and venules without capillary intervention.^{6,8} Hence, we can hypothesize that the AVAs could have an impact on the multifractality of the LDF signals. However, other differences between these two anatomical zones, such as vessel caliber or type and composition of the vessel wall (e.g., muscular vs elastin), could also have an impact on the results obtained. Moreover, our results show that estimated generalized fractal dimensions more curved at scales corresponding to the res-

piration than at scales corresponding to the heart rate. This may indicate that, in the microcirculation, the respiration could be more irregular than the cardiac rhythm. A study, based on a model of approximate entropy, has already obtained similar results, showing that, for healthy subjects, respiration signals are more complex than RR interval signals (heart rate).⁴⁰ Furthermore, from our results, we can suppose that the endothelial and neurogenic mechanisms may have a more irregular behavior in the hand palm than in the forearm. The type of nerve supply could explain the results obtained with the neurogenic mechanism. On the one hand, there is a higher density of tactile receptors in the hand palm. On the other hand, contrary to glabrous skin, the forearm vessels are under cholinergic as well as adrenergic regulation.⁴¹ For the results obtained with the endothelial mechanisms, predominant role of endothelial NO or EDHF in the regulation of microcirculation could bring some explanations. For example, it has been shown that EDHF plays an important role in human forearm circulation *in vivo* in an agonist-specific manner.⁴² More research is needed to investigate the physiological importance of these observations.

VII. SUMMARY AND CONCLUSIONS

Many biological signals were recently analyzed to evaluate their mono- or multifractality. Most of them were recorded from the central cardiovascular system. In this study, we have processed LDF signals that correspond to data issued from the peripheral cardiovascular system. For the first time, the generalized fractal dimensions of signals recorded simultaneously on four different sites (glabrous and nonglabrous zones) were estimated using the partition function. Moreover, the main novelty of the method is the multifractal analysis of data at scales where different FIMFs can be found.

Our results show that LDF signals recorded on the hand palm could be more complex than those recorded on the forearm. Furthermore, spatial variations are more important on the hand palms than on the forearms. Our study also shows that the possible multifractal properties of LDF signals are not mainly governed by a central command. Moreover, showing the generalized fractal dimensions estimated at different scales, we have underlined the possible impact of different mechanisms on the multifractality of the LDF signals.

Using this signal processing method on LDF signals recorded on two different anatomical zones has led to results which seem in concordance with the physiological properties of these zones. These results are very encouraging and could permit one to develop a new LDF signal analyzing method. Thus, it may become possible to study specific FIMF and to observe more precisely the impact of some pathologies on the skin blood flow.

The underlying factors leading to the multifractality of LDF signals are still unknown. However, our findings suggest that the complexity of the signals could depend, among others, on (a) the physiological characteristics of the zone where the LDF signals are recorded and (b) the preponder-

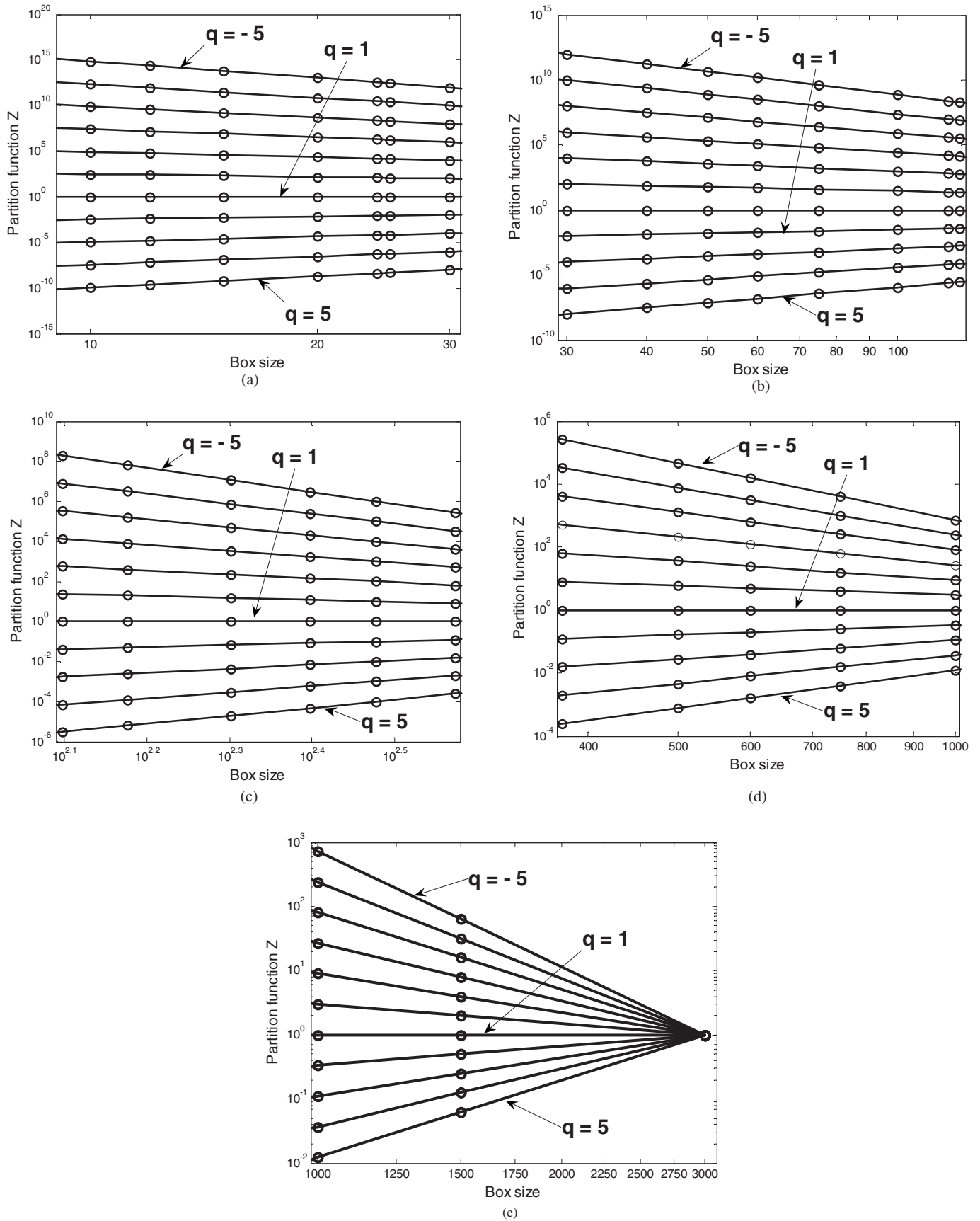


FIG. 7. Zooms of a partition function for the normalized LDF signal recorded in the right forearm of a young healthy subject (29 yr old) in a supine position. The q parameter varies between -5 and 5 . The sizes of the boxes varies between (a) 10 and 30 samples to be in accordance with the cardiac rhythm, (b) 30 and 125 samples for the respiration, (c) 125 and 375 samples for the myogenic mechanisms, (d) 375 and 1000 samples for the neurogenic mechanisms, and (e) 1000 and 3000 samples for the endothelial-related mechanisms.

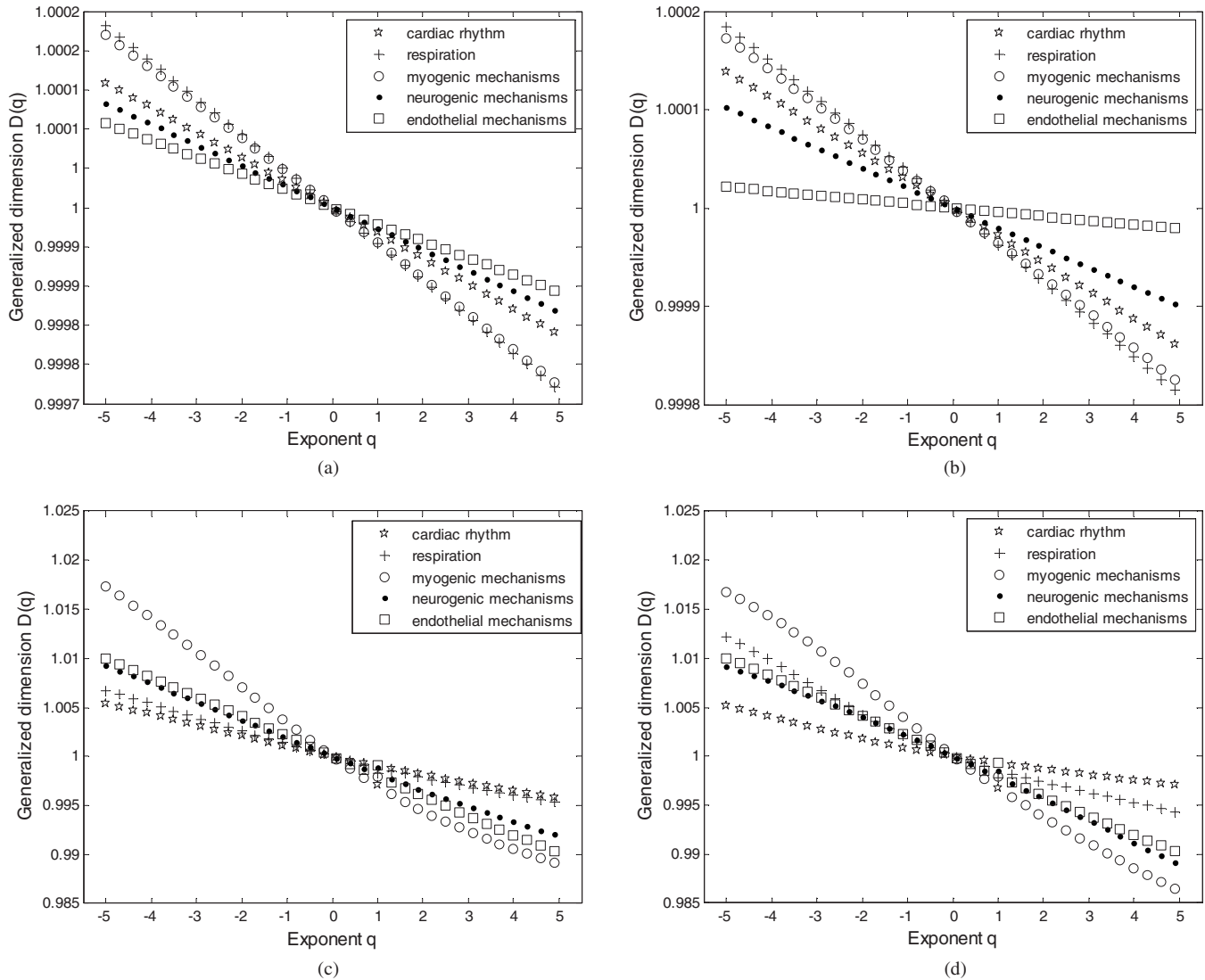


Fig. 8. Average generalized fractal dimensions obtained with the normalized LDF signals recorded (a) in the right forearm, (b) in the left forearm, (c) in the right hand palm, and (d) in the left hand palm of eight healthy subjects in a supine position. The q parameter varies between -5 and 5 . The sizes of the boxes varies between 10 and 30 samples for the cardiac rhythm, between 30 and 125 samples for the respiration, between 125 and 375 samples for the myogenic mechanisms, between 375 and 1000 samples for the neurogenic mechanisms, and between 1000 and 3000 samples for the endothelial-related mechanisms.

ance of some factors according to the studied scales. This study is a first step in order to have more knowledge on the potential implication of different FIMF in the complexity of LDF signals. Further studies are now needed in order to (1) better understand the physiological/anatomical properties of the microcirculation and (2) test our multifractal analysis in different conditions. It would be particularly interesting to observe the results obtained with data recorded in pathological subjects.

ACKNOWLEDGMENT

One of the authors (B.B.) acknowledges support from *La Région des Pays de la Loire*, France.

^{a)}Telephone: +33(0)241966510; Fax: +33(0)241966511; Electronic mail: bbuard@esaip.org

¹M. D. Stern, "In vivo evaluation of microcirculation by coherent light

scattering," *Nature (London)* **254**, 56–58 (1975).
²R. F. Bonner and R. Nossal, "Principles of laser-Doppler flowmetry," in *Laser-Doppler Blood Flowmetry*, edited by A. P. Shepherd and P. A. Oberg (Kluwer Academic, Boston, MA, 1990), pp. 17–45.
³A. Humeau, W. Steenbergen, H. Nilsson, and T. Strömberg, "Laser Doppler perfusion monitoring and imaging: Novel approaches," *Med. Biol. Eng. Comput.* **45**, 421–435 (2007).
⁴G. E. Nilsson, "Signal processor for laser Doppler tissue flowmeters," *Med. Biol. Eng. Comput.* **22**, 343–348 (1984).
⁵J. M. Johnson, G. L. Brengelmann, J. R. Hales, P. M. Vanhoutte, and C. B. Wenger, "Regulation of the cutaneous circulation," *Fed. Proc.* **45**, 2841–2850 (1986).
⁶I. C. Roddie, "Circulation to skin and adipose tissue," in *Handbook of Physiology: The Cardiovascular System*, edited by J. T. Shephard and F. M. Abboud (APS, Bethesda, MD, 1983), pp. 285–317.
⁷D. Wolfenson, "Blood flow through arteriovenous anastomoses and its thermal function in the laying hen," *J. Physiol. (London)* **334**, 395–407 (1983).
⁸K. Lossius, M. Eriksen, and L. Walløe, "Fluctuations in blood flow to acral skin in humans: Connection with heart rate and blood pressure variability," *J. Physiol. (London)* **460**, 641–655 (1993).

- ⁹A. D. M. Greenfield, "The circulation through the skin," in *Handbook of Physiology*, Circulation Vol. II (American Physiological Society, Washington, D.C., 1963), Sec. 2, Chap. 39, pp. 1325–1351.
- ¹⁰S. Yanagimoto, T. Kuwahara, Y. Zhang, S. Koga, Y. Inoue, and N. Kondo, "Intensity-dependent thermoregulatory responses at the onset of dynamic exercise in mildly heated humans," *Am. J. Physiol.* **285**, R200–R207 (2003).
- ¹¹T. E. Wilson, R. Zhang, B. D. Levine, and C. G. Grandall, "Dynamic autoregulation of the cutaneous circulation: Differential control in glabrous vs. non-glabrous skin," *Am. J. Physiol. Heart Circ. Physiol.* **289**, H385–H391 (2005).
- ¹²F. Yamazaki and R. Sone, "Different vascular responses in glabrous and nonglabrous skin with increasing core temperature during exercise," *Eur. J. Appl. Physiol.* **97**, 582–590 (2006).
- ¹³A. Humeau, F. Chapeau-Blondeau, D. Rousseau, M. Tartas, B. Fromy, and P. Abraham, "Multifractality in the peripheral cardiovascular system from pointwise Hölder exponents of laser Doppler flowmetry signals," *Biophys. J.* **93**, L59–L61 (2007).
- ¹⁴A. Humeau, F. Chapeau-Blondeau, D. Rousseau, W. Trzepizur, and P. Abraham, "Multifractality, sample entropy, and wavelet analyses for age-related changes in the peripheral cardiovascular system: Preliminary results," *Med. Phys.* **35**, 717–723 (2008).
- ¹⁵P. Å. Öberg, "Laser-Doppler flowmetry," *Crit. Rev. Biomed. Eng.* **18**, 125–163 (1990).
- ¹⁶R. Freeman, "Assessment of cardiovascular autonomic function," *Clin. Neurophysiol.* **117**, 716–730 (2006).
- ¹⁷P. Kvandal, S. A. Landsverk, A. Bernjak, A. Stefanovska, H. D. Kvernmo, and K.-A. Kirkeboen, "Low-frequency oscillations of the laser Doppler perfusion signal in human skin," *Microvasc. Res.* **72**, 120–127 (2006).
- ¹⁸M. Bračič and A. Stefanovska, "Wavelet-based analysis of human blood-flow dynamics," *Bull. Math. Biol.* **60**, 919–935 (1998).
- ¹⁹A. Stefanovska, M. Bračič, S. Strle, and H. Haken, "The cardiovascular system as coupled oscillators?," *Physiol. Meas.* **22**, 535–550 (2001).
- ²⁰H. D. Kvernmo, A. Stefanovska, M. Bracic, K. A. Kirkerboen, and K. Kvernebo, "Spectral analysis of the laser Doppler perfusion signal in human skin before and after exercise," *Microvasc. Res.* **56**, 173–182 (1998).
- ²¹S. Bertuglia, A. Colantuoni, and M. Intaglietta, "Effects of L-NMMA and indomethacin on arteriolar vasomotion in skeletal muscle microcirculation of conscious and anesthetized hamsters," *Microcirc. Res.* **48**, 68–84 (1994).
- ²²T. M. Griffith and H. Edwards, "Fractal analysis of role of smooth muscle Ca²⁺ fluxes in genesis of chaotic arterial pressure oscillations," *Am. J. Physiol.* **266**, H1801–H1811 (1994).
- ²³J. Kastrup, J. Bühlow, and N. A. Lassen, "Vasomotion in human skin before and after local heating recorded with laser Doppler flowmetry. A method for induction of vasomotion," *Int. J. Microcirc.: Clin. Exp.* **8**, 205–215 (1989).
- ²⁴T. Söderström, A. Stefanovska, M. Veber, and H. Svenson, "Involvement of sympathetic nerve activity in skin blood flow oscillations in humans," *Am. J. Physiol. Heart Circ. Physiol.* **284**, H1638–H1646 (2003).
- ²⁵H. D. Kvernmo, A. Stefanovska, K. A. Kirkerboen, and K. Kvernebo, "Oscillations in the human cutaneous blood perfusion signal modified by endothelium-dependent and endothelium-independent vasodilators," *Microvasc. Res.* **57**, 298–309 (1999).
- ²⁶P. Kvandal, A. Stefanovska, M. Veber, H. D. Kvernmo, and K. A. Kirkeboen, "Regulation of human cutaneous circulation evaluated by laser Doppler flowmetry, iontophoresis and spectral analysis: Importance of nitric oxide and prostaglandins," *Microvasc. Res.* **65**, 160–171 (2003).
- ²⁷B. B. Mandelbrot, "Intermittent turbulence in self-similar cascades: Divergence of high moments and dimensions of the carrier," *J. Fluid Mech.* **62**, 331–358 (1974).
- ²⁸T. C. Halsey, M. H. Jensen, L. P. Kadanoff, I. Procaccia, and B. I. Shraiman, "Fractal measures and their singularities—The characterization of strange sets," *Phys. Rev. A* **33**, 1141–1151 (1986).
- ²⁹P. Grassberger, "Generalized fractal dimensions of strange attractors," *Phys. Lett. A* **97**, 227–230 (1983).
- ³⁰P. Ch. Ivanov, A. L. Goldberger, and H. E. Stanley, in *The Science of Disasters*, edited by A. Bunde, J. Kropp, and H.-J. Schellnhuber (Springer, Berlin, 2002), pp. 219–257.
- ³¹A. Humeau, B. Buard, F. Chapeau-Blondeau, D. Rousseau, G. Mahé, and P. Abraham, "Multifractal analysis of central (electrocardiography) and peripheral (laser Doppler flowmetry) cardiovascular time series from healthy human subjects," *Physiol. Meas.* **30**, 617–629 (2009).
- ³²J. Feder, *Fractals* (Plenum, New York, 1988).
- ³³J. M. Diego, E. Martinez-Gonzales, J. L. Sanz, S. Mollerach, and V. J. Martínez, "Partition function based analysis of cosmic microwave background maps," *Mon. Not. R. Astron. Soc.* **306**, 427–436 (1999).
- ³⁴N. Sarkar and B. B. Chaudhuri, "Multifractal and generalized fractal dimensions of gray-tone digital images," *Signal Process.* **42**, 181–190 (1995).
- ³⁵H. Takayasu, *Fractals in the Physical Sciences* (Manchester University Press, Manchester, 1997).
- ³⁶C. J. G. Evertsz and B. B. Mandelbrot, "Multifractal measures," in *Chaos and Fractals*, edited by H. O. Peitgen, H. Jürgens, and D. Saupe (Springer, Berlin, 1992), pp. 921–953.
- ³⁷H. Takayasu, "Differential fractal dimension of random walk and its applications to physical systems," *J. Phys. Soc. Jpn.* **51**, 3057–3064 (1982).
- ³⁸M. A. López-Quintela, J. C. Pérez-Moure, M. C. Buján-Núñez, and J. Samios, "Influence of fractal dimension on diffusion-controlled reactions," *Chem. Phys. Lett.* **138**, 476–480 (1987).
- ³⁹B. Buard, G. Mahé, F. Chapeau-Blondeau, D. Rousseau, P. Abraham, and A. Humeau, "Étude des variations spatiales des spectres multifractals de signaux laser Doppler," OPT-DIAG Symposium on Diagnostic and Optical Imagery in Medicine, Paris, France, 2009 (unpublished).
- ⁴⁰J. Peupelmann, M. K. Boettger, C. Ruhland, S. Berger, C. T. Ramachandrarajah, V. K. Yeragani, and K.-J. Bär, "Cardio-respiratory couplings indicates suppression of vagal activity in acute schizophrenia," *Schizophr Res.* **112**, 153–157 (2009).
- ⁴¹J. M. Johnson, "Circulation to the skin," in *Textbook of Physiology*, 21st ed., edited by H. D. Patton, A. F. Fuchs, B. Hille, A. M. Scher, and R. Steiner (WB Saunders, Philadelphia, PA, 1989), pp. 898–910.
- ⁴²K. Inokuchi, Y. Hirooka, H. Shimokawa, K. Sakai, T. Kishi, K. Ito, Y. Kimura, and A. Takeshita, "Role of endothelium-derived hyperpolarizing factor in human forearm circulation," *Hypertension* **42**, 919–924 (2003).